

Structural, Electrical and Magnetic Properties of High Iron Content Sodium Borosilicate Glass

M. M. Eltabey^{1, 2}, H. A. Othman³, Samia. E. Ibrahim³,
L.M. Sharaf El-Deen³, M.M. Elkholy³

¹Basic Engineering Science Department, Faculty of Engineering, Menoufiya University, Shibin El-Koom, Egypt.

²Preparatory Year Deanship, Science Department -Physics, Jazan University, Saudi Arabia.

³Physics Department, Faculty of Science, Menoufiya University, Shibin El-Koom, 32511, Menoufiya, Egypt

Abstract: A series of high iron content sodium borosilicate glasses having composition $10 \text{ SiO}_2\text{-}40 \text{ B}_2\text{O}_3\text{-}50 \text{ Na}_2\text{O}\cdot x \text{ (CoO-Fe}_2\text{O}_3)$; $0 \leq x \leq 50 \text{ wt}\%$ were prepared by conventional melt quench method. Density of these glasses was found to increase in the range of 2.47-3.03 g/cm³, along with increasing glass molar volume. FTIR showed the gradual conversion of BO_3 units to BO_4 units along with enhanced B-O-Si linkage with the increasing of $\text{(CoO-Fe}_2\text{O}_3)$ content. AC electrical conductivity and dielectric properties were investigated at room temperature within frequency range 100 Hz to 100 KHz. Dielectric parameters such as dielectric constants ϵ' and ϵ'' with the ac. conductivity σ_{ac} were found to increase with increasing of $\text{(CoO-Fe}_2\text{O}_3)$ content. The increase in ac conductivity with iron content is likely to arise due to structural changes of the glass network. Magnetic hysteresis loops were traced at room temperature using VSM and values of saturation magnetization M_s and coercive field H_C were determined. The obtained results revealed that a ferrimagnetic behavior was observed and as $\text{(CoO-Fe}_2\text{O}_3)$ concentration increases the values of M_s increase whereas that of H_C dramatically decreased from 271.12 to 179.23 Oe.

Keywords: Boro-Silicate glass; Electrical properties; Magnetic properties; Structure.

I. Introduction

Borosilicate glasses based on the $\text{Na}_2\text{O-B}_2\text{O}_3\text{-SiO}_2$ system play a significant role in various applications, ranging from chemically and thermal resistant technical glass to optical, sealing and nuclear waste glasses [1]. It is well known that, borosilicate glasses have mixed network formers and combine the advantages of the stability of silicate glass and the higher transition metal (TM) ion solubility of borate glass without producing heavy concentration quenching, and thus are promising candidates for good TM ion hosts [2]. In the past few decade, glasses doped with transition metal oxides have attracted a great deal of attention due to their important physical and chemical properties [3- 4].

LONG-TERM storage of nuclear waste has become an important application of borosilicate glasses. In this use, however, the physical properties of the borosilicate matrix can be modified by the elements to be stored, many of which (Ce, Fe, ...) are multivalent [5].

The nuclear waste often contain many non-radioactive components such as Fe and may vary widely composition. Glass composition that could bear high iron content without crystallization hence is a candidate for nuclear waste storage. In particular, Fe_2O_3 has been considered as one of the most promising candidate for improving physical properties of glasses such as electrical, optical and magnetic properties [6,7]. Because iron lends itself readily to experimental investigation, we have examined how the structure of a sodium borosilicate glass is affected by iron content. It was shown that the magnetic and electrical properties of prepared glass are highly affected by $\text{(CoO-Fe}_2\text{O}_3)$ additive. The improved chemical durability of phosphate glasses system is caused by the addition of Fe_2O_3 which strengthens the cross bonding between the phosphate chains [8]. In addition, glass doped with multivalent ions, such as Fe^{3+} and Co^{3+} , have been used for many applications, such as semiconducting glass, active oxide catalysts to oxidize Co and hydrocarbons, and glassy behavior in manganites [9, 10].

The main problem associated with the synthesis of oxide glasses with high concentrations of transition metals using standard melting techniques is that the corresponding products may crystallize spontaneously [11-15].

The main objective of the present work is to prepare iron and cobalt rich glass without crystallization in order to study the effect of high $\text{(CoO-Fe}_2\text{O}_3)$ content on the physical properties of the prepared glass. Such glasses are expected to possess magnetic and electrical properties that are of significant importance in many technological applications at room temperature such semiconducting glass and nuclear waste.

II. Experimental Technique

2.1 Samples Preparation

The glass system 10 SiO₂-40 B₂O₃-50 Na₂O : x (CoO-Fe₂O₃); 0 ≤ x ≤ 50 wt% was prepared by melting dry mixtures of analytical grade chemicals of SiO₂, B₂HO₃, Na₂CO₃, CoO, Fe₂O₃. The oxides used herein were analytical reagent grade (more than 99% pure). The raw materials were weighed using an electronic balance with accuracy on order of 0.1 mg. Approximately 15 g of chemicals good mixed in a porcelain crucible. The glass melt was kept at 1150 °C for approximately 30 min, for complete fusion of the glass. Glass sample was obtained by casting the melt on a steel plate.

2.2 Density And Molar Volume Measurements

The density (ρ_g) of the glasses was determined at room temperature using Archimedes' principle with toluene (density = 0.867 g/ml at 20°C) as buoyant liquid. The density of each glass was obtained according to the formula,

$$\rho_g = \left(\frac{W_a}{W_a - W_t} \right) \times \rho_t \quad (1)$$

Where ρ_g the density of the sample, W_a the weight of the sample in air, W_t the weight of the sample in toluene, and ρ_t the density of toluene. The molar volume (V_m) of each glass sample was calculated using the formula,

$$V_m = \frac{\sum X_i M_i}{\rho_g} \quad (2)$$

Where, X_i is the molar fraction and M_i is the molecular weight of the i^{th} component. The reproducibility of the density data obtained was no worse than $\pm 0.01 \text{ g cm}^{-3}$.

2.3 X-ray diffraction

XRD patterns of the prepared glasses were obtained by grounding small pieces of them in an agate mortar to obtain very fine powder. The structure of the samples have been investigated by using (BRUKUR D8ADVANCE) provided with Cu-K α target of a wavelength $\lambda = 1.542 \text{ \AA}$. XRD patterns were recorded in the diffraction range $2\theta = 4-80^\circ$ with a step of 0.03° .

2.4 IR transmission spectra

The measurements of IR transmission spectra wererecorded at room temperature by the KBr disk method using an FTIR spectrophotometer type Tensor 27, Brulear over the wave number $4000-200 \text{ cm}^{-1}$.

2.5 Electrical properties measurements

Room temperature electric measurements were carried out using (Hioki 3520 LCR HiTester Meter Bridge) in the frequency range of 100 Hz-100 kHz. For good electrical contact during measurements, the opposite sides of the bulk samples were painted with silver paste. By using the measured values of capacitance C, dielectric loss factor δ and dimensions of the samples we have calculated the dielectric constant, ϵ' , dielectric loss, ϵ'' , and ac conductivity, σ_{ac} , using following expressions

$$\epsilon' = \frac{Cd}{\epsilon_0 A} \quad (3)$$

$$\epsilon'' = \epsilon' \tan \delta \quad (4)$$

$$\sigma_{ac} = \frac{d}{ZA} \quad (5)$$

Where, ϵ_0 is the dielectric constant of the free space ($8.854 \times 10^{-9} \text{ F/cm}$), d is the thickness, A is cross sectional area of the sample and Z is the impedance.

2.6 Magnetic properties measurements,

Room temperature magnetic measurements were carried out using the Lake-Shore vibrating sample magnetometer (VSM) model 7410. Hysteresis loops were traced in a magnetizing range from -15000 to 15000 G and values of saturation magnetization M_S and coercive field H_C were determined automatically.

III. Results And Discussion

3.1 X-Ray Diffraction Analysis

X-ray diffraction (XRD) spectra of all investigated glasses are shown in Fig. 1(a,b). All samples were found to be in glassy form. For the sample with the highest concentration of (CoO-Fe₂O₃) 50 wt%, it was observed a crystalline diffracted line, especially the more intense one, (311) plane for the spinel cubic structure, at angle about $2\theta \approx 35^\circ$, combined with the hump of the glass structure.

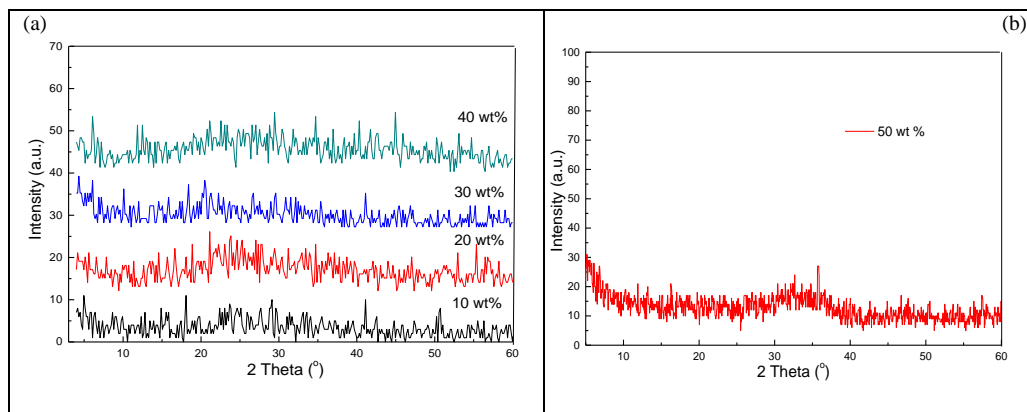


Fig.1 X-ray diffraction patterns for 10 SiO₂-40 B₂O₃-50 Na₂O: x (CoO-Fe₂O₃) glasses

3.2 Density Measurements

Fig. 2 shows the variations of the density (ρ_g) and molar volume (V_m) with wt % of (CoO-Fe₂O₃) content this figure indicates that the glass density is increased gradually from 2.47 to 3.03 g/cm³ and the molar volume also, increased from 33.91 to 66.35 cm³ as the (CoO-Fe₂O₃) content is increased up to 50 wt %, almost in a linear behavior.

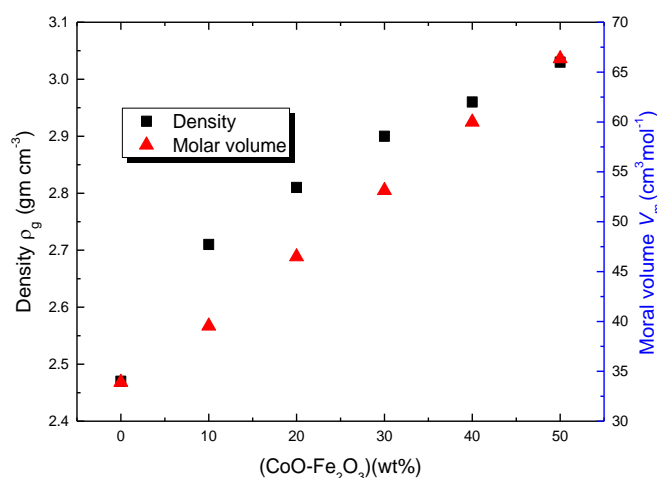


Fig. 2. Variation of density and molar volume as a function of composition of the prepared glass.

The increase of both density and molar volume could be attributed to an increase of the average molecular weight of oxide ions in the glass due to that, both CoO and Fe₂O₃ have a higher relative molecular mass. The molar volume depends on both the changing rate of density and molecular weight. However, when the (CoO-Fe₂O₃) concentration was increased, the increasing rate of molecular weight is greater than the increasing rate of density. As shown in Fig. 2, the molar volume increased with increasing of Fe₂O₃ content, this is attributed to an increase in the number of non-bridging oxygen (NBOs). The obtained results indicated that the CoO and Fe₂O₃ could enter in the glass network and acted as a modifier by occupying the interstitial space in the network and generating the NBOs to the structure. It was observed that the addition of Fe₂O₃ might accordingly result in an extension of glass network [16]. These structural changes are confirmed by the obtained FTIR spectra.

3.3 Infrared Measurements

IR spectra of the prepared samples are shown in Fig. 3 the spectra are characterized by seven main absorption peaks. Due to low SiO_2 content in the present samples the spectra is dominated by the borate network finger print. The absorption peak in the far infrared region around 320 cm^{-1} is attributed to Fe-O and Co-O vibrations. Another peak in the far infrared region at about 460 cm^{-1} is related to Fe-O bonds stretching vibrations in FeO_6 units [17]. The absorption peak at 700 cm^{-1} is attributed to the bending vibrations of B-O-B linkage in borate network [18]. It was observed that, the intensity of this peak increased with increasing ($\text{CoO-Fe}_2\text{O}_3$) content.

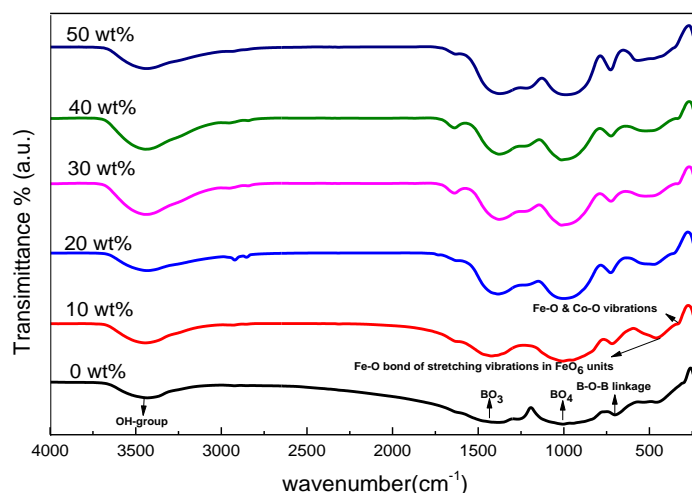


Fig. 3 IR spectra of the prepared samples

The two broad absorption bands in the mid IR region around 950 and 1350 cm^{-1} are assigned to BO_4 and BO_3 units respectively. The first band that extends from 840 to 1140 cm^{-1} is assigned to the B-O stretching vibrations in BO_4 units from diborate, tri-, tetra- and penta-borate groups [18] with overlapped absorption of Si-O-Si network vibrations that give rise to absorption near 815 cm^{-1} . The intensity of the BO_4 units related band increases and shifts toward higher wavenumbers with increasing ($\text{CoO-Fe}_2\text{O}_3$) content. The second band that extends from 1250 to 1490 cm^{-1} is assigned to B-O asymmetric stretching vibrations of BO_3 units in pyro- and ortho-borate groups with overlapped absorption of the stretching vibration of B-O-Si linkage centered around 1120 - 1150 cm^{-1} . It is observed that the intensity of this band showed a little decrease and it shifted toward lower wavenumbers with increasing ($\text{CoO-Fe}_2\text{O}_3$) content. It could be concluded from the previous discussion about the shape and the intensity of the two bands that, the BO_3 bonds convert to BO_4 with the increase in ($\text{CoO-Fe}_2\text{O}_3$) content as the metal cation makes chains with BO_3 which converts it to BO_4 units. The conversion of BO_3 to BO_4 leads to more open structure, which is confirmed, from the observed increase in the molar volume Fig. 2. Si-O-Si network vibrations absorption near 815 cm^{-1} , the absorption intensity in this region decreases with increasing the stretching vibration of B-O-Si linkage absorption around 1120 - 1150 hence we could conclude that with the conversion of BO_3 units to BO_4 units the Si-O-Si network converted to B-O-Si linkage. The absorption peak around 1600 cm^{-1} is assigned to asymmetric stretching relaxation of B-O bonds of trigonals BO_3 units [17]. The absorption peak around 3400 cm^{-1} is assigned to OH group [18].

3.4 Electrical Properties

The frequency dependence of dielectric constant, ϵ' and ϵ'' of 10 SiO_2 - $40 \text{ B}_2\text{O}_3$ - $50 \text{ Na}_2\text{O}$: $x (\text{CoO-Fe}_2\text{O}_3)$; $0 \leq x \leq 50 \text{ wt} \%$ glass system is shown in Figs. 4 and 5 .

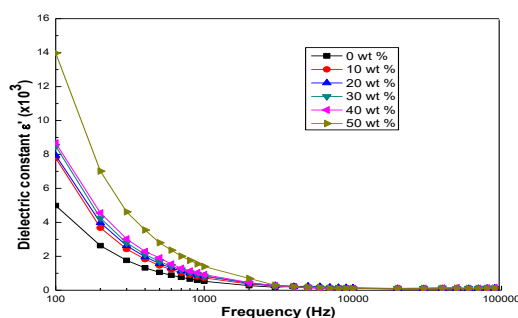


Fig. 4 Frequency dependence of the dielectric constant for the investigated samples at room temperature.

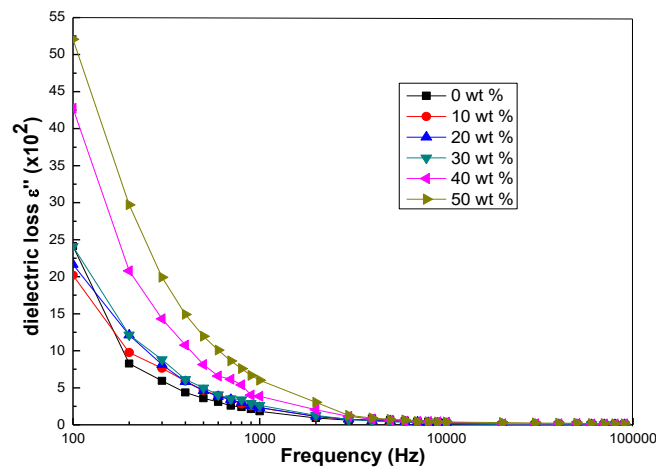


Fig. 5 Frequency dependence of the dielectric loss for the investigated samples at room temperature.

It can be observed that, values of ϵ' decrease with frequency up to a certain frequency and beyond that frequency they remain almost constant. This behavior could be interpreted in terms of the presence of permanent electrical dipoles in the glass that were produced due to the charge pairs formed by the iron ions and non-bridging oxygen. Where at low frequency, where these dipoles can match the frequency of the applied field, the values of ϵ' are maximum. By increasing the frequency of the applied field, these dipoles cannot follow the alternating field and so the values of dielectric constant decrease. Similarly, the decrease of the imaginary part of dielectric constant ϵ'' (which represents the dielectric loss) frequency could be interpreted as follows. Due to the relaxation of these dipoles its orientations, especially at high frequency, cannot follow the applied field frequency.

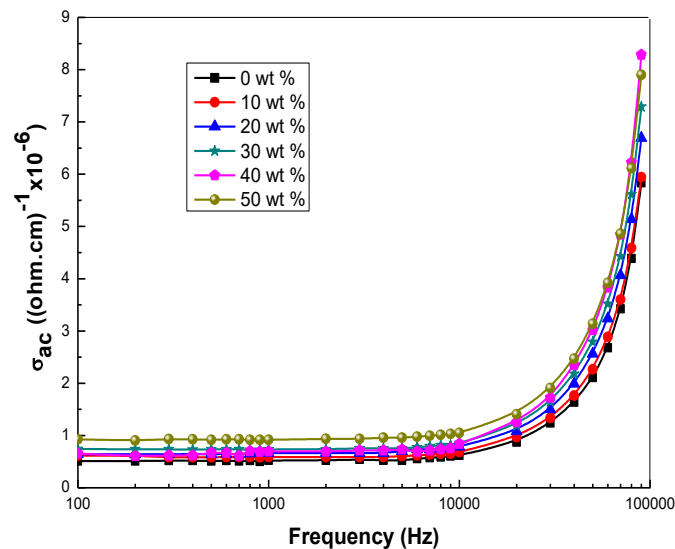


Fig. 6 Frequency dependence of ac conductivity σ_{ac} for the studied samples at room temperature.

Fig. 6 illustrates the frequency dependence of ac conductivity $\sigma_{ac}(\omega)$ of the glass system. The figure shows that the conductivity obeys a power relation, $\sigma_{ac}(\omega) = A \omega^s$, where A is a constant depends on temperature and s is the frequency exponent.

Fig.7 shows the composition dependence of dielectric constants ϵ' and ϵ'' with σ_{ac} at (frequency=300 Hz) for the investigated samples. It is clear that, all of ϵ' , ϵ'' and σ_{ac} are almost increase as the (CoO-Fe₂O₃) wt% content increases. The variation of dielectric constants ϵ' and ϵ'' with composition could be, also, discussed in terms of the presence of permanent electric dipoles in the glass. As the iron concentration increases, more of these permanent dipoles will be arise to share in the polarization leading to increase the values of both ϵ' and ϵ'' with (CoO-Fe₂O₃) content .

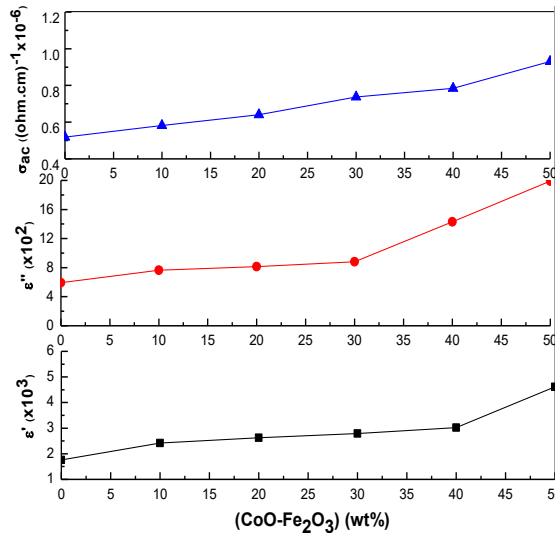


Fig. 7 Composition dependence of dielectric constant ϵ' , ϵ'' and σ_{ac} for the investigated samples at (frequency = 300 Hz).

The increase in ac conductivity with (CoO-Fe₂O₃) wt % concentration presented in Fig. 7 could be explained in view of the structural changes occurring in the glass network. IR and molar volume measurements of this system revealed that the addition of (CoO-Fe₂O₃) to SiO₂-40 B₂O₃-50 Na₂O: x (CoO-Fe₂O₃) glass system increases the number of non-bridging oxygen atoms. Such a creation of non-bridging oxygen leads to open the network and to weak the structure. Therefore, the conductivity increase could be attributed to the increase of mobility of iron ions .

3.5 Magnetic properties

Room temperature M-H loops for all the investigated samples are shown in Fig. 8. One can easily observe two notes for all the measured samples. Frist, the loops are open hysteresis loops. Second, there is nearly a full saturation behavior observed especially at the high values of magnetizing field. These observations revel and indicate to the presence of an ordered magnetic structure [19, 20]. This result supports that obtained from the x-ray diffraction .Where, it was observed a crystalline diffracted lines at the highest concentration of (CoO-Fe₂O₃), especially the more intense one (311) plane at angle about $2\theta \approx 35^\circ$, combined with the hump of the glass structure. So, one can note that, although there was no crystalline lines are observed in the diffraction patterns especially at low concentrations of (CoO-Fe₂O₃), the magnetic measurements could indicate the formation of ordered phase.

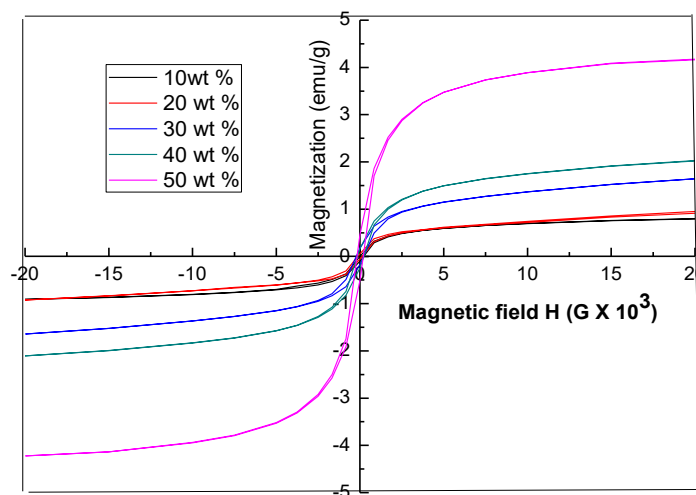


Fig.8 Hysteresis loops of the 10 SiO₂-40 B₂O₃-50 Na₂O: x (CoO-Fe₂O₃) glass system

The dependence of saturation magnetization M_S , determined by extrapolation of the magnetization curve to $H=0$, on (CoO-Fe₂O₃) concentration is illustrated in Figure9. It is obvious that as the concentration of (CoO-Fe₂O₃) increases, the values of M_S are continually increases. This trend could be attributed to that, as the

weight percentage (wt %) of (CoO-Fe₂O₃) increases the concentration of ferrimagnetic phase, the ordered one, in the prepared samples increases. This leads to increase the number of magnetic moments per unit volume which is called magnetization.

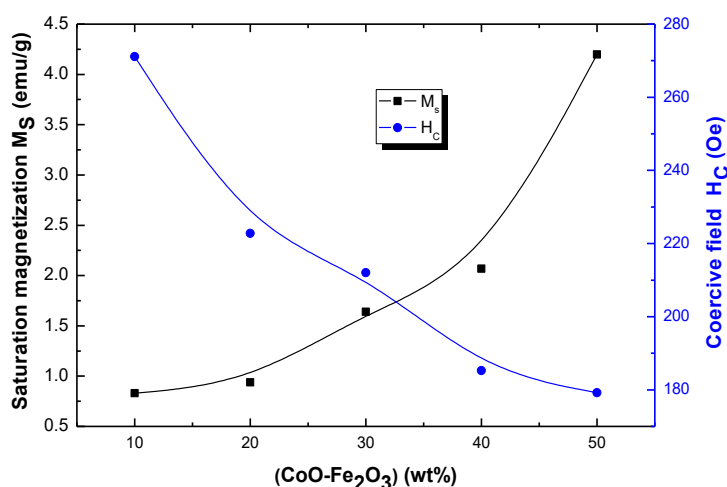


Fig. 9: Variation of saturation magnetization M_s (emu/g) and coercive field H_c (Oe) with (CoO-Fe₂O₃) concentration (Wt %)

Fig.9 shows also the change of the coercive field (H_c) with (CoO-Fe₂O₃) –concentration. It is obvious that H_c decreases dramatically with increasing (CoO-Fe₂O₃) content. This behavior could be explained in light of Brown's relation. Where, the coercivity depends upon particle size, saturation magnetization M_s and magnetocrystalline anisotropy constant (k₁). Brown's relation is given by,

$$H_c \approx \frac{2K_1}{\mu_0 M_s} \quad (6)$$

where, μ_0 is the magnetic permeability. It is known that the anisotropy field in ferrites results mainly from the presence of Fe²⁺ ions [21, 22]. Since the ferrimagnetic phase which is formed is CoFe₂O₄ for all the investigated samples, then the concentration of Fe²⁺ ions is almost constant leading to make K₁ is the same for all the samples. Thus, according to Brown's relation, as (CoO-Fe₂O₃) concentration increases the values of M_s increases leading to decrease the values of H_c which is obtained in the results.

IV. Conclusion

Addition of (CoO-Fe₂O₃) to the glass system 10 SiO₂-40 B₂O₃-50 Na₂O: x (CoO-Fe₂O₃) leads to:

- Gradual increase of the density because of the high molecular weight of Fe and Co ions.
- The conversion of BO₃ units to BO₄ units results in an increased molar volume of the studied glass system. A slower rate of molar volume increase at high (CoO-Fe₂O₃) content is attributed to enhanced B-O-Si linkage.
- Dielectric parameters such as dielectric constants ϵ' , ϵ'' , and a.c. conductivity σ_{ac} were found to increase with increasing of (CoO-Fe₂O₃) content.
- Formation of nano-crystalline particles of CoFe₂O₄ ferrite phase.
- Increase the values of saturation magnetization and decrease that of coercive field.

References

- [1]. Ehrhart Doris, Keding Ralf, Phys. Chem. Glasses: Eur. J. Glass Sci. Technol. B, June 2009, 50 (3), 165–171.
- [2]. Wena Hongli, Peter A. Tanner, Journal of Alloys and Compounds 2015, 625, 328–335.
- [3]. A. Mekki, G. D. Khatak, D. Holland, M. Chinkhota, and L. E. Wenger, J. Non-Cryst. Solids 2003, 318 -193.
- [4]. N. Zotov, A. Kirfel, B. Beuneu, R. Delaplane, D. Hohlwein, F. Reinauer, and R. Glaum, Physica B 2004, 350, 1071.
- [5]. B. Cochain, D. R. Neuville, G. S. Henderson, A. Mc Cammon, k O. Pinet, and P. Richet, J. Am. Ceram. Soc. 2012, 95 (3), 962–971.
- [6]. V. Licina, A. Mogus-Milankovic, S. T. Reis, D. E. Day, J. Non-Cryst. Solids 2007, 353, 4395.
- [7]. L. Ardelean, R. Lungu, and P. Pacuta, J. Mater Sci. 2007, 18, 837.
- [8]. A.M. Milankovic, B. Pivac, K. Furic, D.E. Day, Phys. Chem. Glasses 1997, 38 (2), 74.
- [9]. J. Mao, M. Y. Sui, X. Wang, Yiyun Yang, Zhang, X. Wang, Yang Wang, Y. W. Liu, J. Alloys Compd. 2011, 509, 4950–4953.
- [10]. H. Tran, T. Mehta, M. Zeller, R.H. Jarman, Mater. Res. Bull. 2013 , [http:// dx. doi.org/10.1016/j. mater res bull. 2013, 02, 060](http://dx.doi.org/10.1016/j.mater.res.bull.2013.02.060).

- [11]. M. Romero, J.M. Rincon, J. Am Ceram Soc. 1999, 82-1313.
- [12]. D. Ehrhart, H. Rei, W. Vogel, Silikattechnik 1976, 27-304.
- [13]. H.J.L. Trap, J.M. Stevels, Phys. Chem. Glasses 1963, 4-193.
- [14]. R. Harizanova, G. Volksch, C. Russel, J. Mater. Sci. 2010, 45-1350, doi:10.1007/s10853-009-4090-7.
- [15]. R.; Harizanova, R. Keding, G. Volksch, C. Russel, Eur. J. Glass Sci. Technol. 2008, 49-177.
- [16]. J. Kaewkhao, W. Siriprom, S. Insiripong, T. Ratana, C. Kedkaew, and P. Limsuwan, Journal of Physics 2015 Conference Series 2011, 266,012012.
- [17]. Semiconductor Physics, Quantum Electronics & Optoelectronics, 2008, 11(3), 221-225.
- [18]. International Scholarly Research Network, ISRN Ceramics, 2012, Article ID 428497, 17, doi:10.5402/2012/428497.
- [19]. B. Issa, I. M. Obaidat, B. A. Albiss, and Y. Haik, International Journal of Molecular Sciences 2013 14, (11), 21266–21305.
- [20]. M. M. Eltabey, A. M. Massoud, and Cosmin Radu, Journal of Nanomaterials, 2014, Article ID 492832, 7 pages.
- [21]. A.A. Sattar, H.M. El-Sayed, K.M. El-Shokrofy, and M.M. Eltabey, Journal of Applied Sciences 2005, 5 (1), 162-168.
- [22]. A.M. Wahba, Ali N. Aboufotouh, M. M. Eltabey, Materials Chemistry and Physics, 2014, 146 (3), 224-229.